

## Dynamics of Weakly Connected Solids: Silica Aerogels

D. W. Schaefer and C. J. Brinker

*Sandia National Laboratories, Albuquerque, New Mexico 87185*

D. Richter, B. Farago, and B. Frick

*Institut Laue-Langevin, 38042 Grenoble, France*

(Received 13 November 1989)

Applying neutron spin-echo spectroscopy, we investigate low-energy vibrational excitations in a series of silica aerogels of varying connectivity. Connectivity is adjusted both by precursor solution chemistry and by heat treatment. Polymeric aerogels show fractonlike densities of states, whereas colloidal materials exhibit a peak in the  $\mu\text{eV}$  regime. On sintering, the low-frequency excitations disappear. We conclude that neutron spin-echo spectroscopy provides a measure of the topological aspects of disordered materials.

PACS numbers: 82.70.-y, 61.41.+e, 63.50.+x

The nature of vibrational excitations in amorphous materials remains one of the central unsolved problems of solid-state physics.<sup>1</sup> These materials consistently show anomalous low-temperature properties indicative of low-energy excitations absent in crystalline analogs. Just as some understanding of these phenomena emerged for dense materials,<sup>2,3</sup> evidence for an entirely new class of vibrational excitations appeared for porous, weakly connected solids.<sup>4-7</sup> These new excitations appear at exceedingly low energy, making them directly accessible only by very-high-resolution techniques. Here we characterize a variety of porous silica aerogels using neutron spin-echo (NSE) spectroscopy, the highest-resolution spectroscopy currently available.<sup>8</sup>

The new class of excitations we seek are network, as opposed to local, excitations. In tenuous solids, these modes are sensitive to the long-range connectivity rather than to local interatomic potentials. For self-similar or fractal networks, recent theoretical work<sup>9,10</sup> suggests that the vibrational density of states (DOS)  $g(\omega)$  is particularly simple,

$$g(\omega) \sim \omega^{d-1}, \quad (1)$$

where  $d$  is the so-called spectral or fracton dimension. Since  $d$  is directly dependent on the network connectivity (branching), vibrational spectroscopy, in principle, provides a unique tool to measure this elusive feature of networks. Porous silica aerogels are often fractal<sup>11</sup> so they represent an ideal system on which to evaluate these new concepts.

The goal of our work is to measure the frequency dependence of the DOS for solids of differing connectivity. We therefore exploited existing ideas on the dependence of connectivity on synthetic protocol of the solution precursors to prepare several classes of silica aerogels. In addition, we used thermal treatment to modify connectivity with and without simultaneous disruption of long-range fractal correlations.

By comparing small-angle scattering (SAS) and NSE

data, we show that fracton dynamics are characteristic of polymeric aerogels (samples *A-C*), whereas for the colloidal aerogel (*D*) a peaked DOS is observed, albeit centered at exceedingly low energies. We emphasize that our data indicate qualitative changes in the form of the DOS, not just changes in  $d$ .

Our work benefits from the pioneering work of others who have used Raman,<sup>5,12</sup> Brillouin,<sup>13</sup> and neutron scattering<sup>12,14-16</sup> to investigate aerogel dynamics. In general, comparison with these studies is difficult because of different energy regimes, multiphonon scattering, different preparation recipes, and questions concerning what is actually measured by optical methods. It appears, however, that our results differ substantially from previous conclusions.

*Structure and connectivity.*—To investigate the relationship between vibrational excitations, structure, and connectivity we prepared a series of samples in which structure and connectivity differ. Structure can be assessed directly by SAS. In the absence of definitive methods to determine network connectivity, however, we rely on models for solution polymerization of precursors to give at least a qualitative guide to connectivity. We studied materials with both polymeric and colloidal microstructures. Finally, we heat treated the polymeric materials, first increasing local connectivity but leaving the long-range network intact (pyrolysis) and then further enhancing branching with concurrent destruction of the fractal network (sintering).

In all cases, NSE requires the minimization of incoherent scattering which arises primarily from hydrogen. Two of our polymeric samples (*A* and *B*) were therefore prepared from completely deuterated precursors. These samples were subjected to a maximum temperature of 200°C, substantially less than the  $\sim 350^\circ\text{C}$  required to pyrolyze the organic groups that stabilize the network. Colloidal (*D*), pyrolyzed (*C*), and sintered samples (*E*) were hydrogenated but subjected to 500°C to eliminate organics. All samples were exchanged with

D<sub>2</sub>O prior to a final 150°C anneal designed to eliminate mobile adsorbed species.

Polymeric aerogels were prepared via a two-state protocol.<sup>17</sup> Tetraethoxysilane was first hydrolyzed in acid solution and then condensed under basic conditions. SAS shows that this procedure leads to polymeric gels<sup>18</sup> and aerogels.<sup>19,20</sup> SAS from the aerogel (curve *A*, Fig. 1) indicates that some collapse of the network occurred on supercritical drying<sup>20</sup> since the Porod slope is 15% steeper than that of the solution precursor.

We increase branching of the above aerogel by pyrolysis (thermal decomposition of organics) of a hydrogenated analog at  $T=500^\circ\text{C}$  for 2 h under N<sub>2</sub>. Pyrolysis of blocking ethoxy groups leads to increased cross-linking at the molecular level consistent with the increased SAS slope (*C*) at  $Q \approx 0.1 \text{ \AA}^{-1}$ . Sintering (high-temperature annealing) of the two-stage sample at 950°C for 20 h leads to a locally dense structure and complete destruction of the fractal network (curve *E*, Fig. 1).

A second polymeric material was prepared from tetramethoxysilane neutrally polymerized in one step ( $\text{pH} \sim 7.5$ ). Here the aerogel (curve *B*, Fig. 1) gives  $D=2.9$  whereas the solution precursor gives  $D=2.5$ , again indicative of some collapse during drying. The connectivity of these materials is believed to be that of a threshold-percolation cluster arising via a process dubbed kinetic percolation.<sup>11</sup>

The two polymeric samples (*A* and *B*) represent ma-

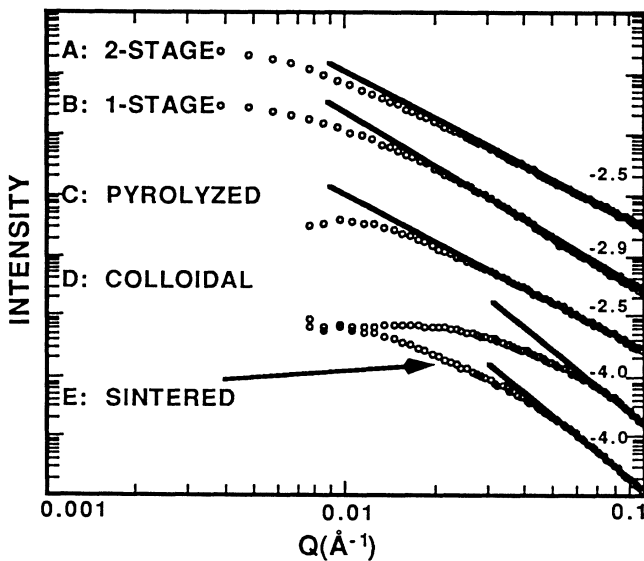


FIG. 1. Small-angle scattering profiles for aerogels. Data were taken on the 10-m small-angle x-ray-scattering instrument at Oak Ridge National Laboratory and the low- $Q$  diffractometer at Los Alamos National Laboratory. Slopes less than  $-3$  indicate colloidal microstructure whereas slopes greater than  $-3$  indicate a polymeric microstructure. The solution precursor of *C* was half the concentration of *A*.

terials of similar structure but different connectivities. The single-stage aerogel should be more ramified (branched) compared to the two-stage one. Indeed, our results are consistent with this hypothesis. To prevent restructuring, materials were maintained below 60°C throughout synthesis, solvent exchange (CO<sub>2</sub>), and supercritical extraction.<sup>20</sup>

An aerogel with a colloidal (particulate) microstructure was obtained from AIRGLASS AB (Staffenstorp, Sweden). This material shows a limiting Porod slope near  $-4$ , the signature of smooth surfaces on short scales (curve *D*, Fig. 1). This material is prepared under basic conditions where early solution growth generates colloidal particles.<sup>19</sup> High-temperature supercritical extraction ( $T=300^\circ\text{C}$ ) leads to further coarsening. The dry aerogel was pyrolyzed at 500°C under N<sub>2</sub> to remove residual organics.

*Inelastic neutron scattering.*—All of the samples were studied using the INII NSE spectrometer at the Institut Laue-Langevin. Data were taken in the time ( $t$ ) domain at  $Q=1.55 \text{ \AA}^{-1}$ , the first peak in the structure factor of amorphous silica. The  $T$  dependence of the normalized intermediate scattering function  $S(Q,t)/S(Q,0)$  was studied between  $T=4$  and 300 K. The data were resolution corrected via elastic scattering from dense amorphous silica. Scattering from the empty Al can was negligible.

Assuming a sound-wave form factor [ $Q^2S(Q)$ ], the multiphonon terms in  $S(Q,t)$  can be summed analytically in the harmonic approximation to give<sup>21</sup>

$$S(Q,t)/S(Q,0) = \exp\{-2W(Q)S(Q)[1 - \gamma(t)]\}, \quad (2)$$

where

$$\gamma(t) \sim \int n(\omega)g(\omega)\exp(i\omega t)d\omega, \quad (3)$$

$n(\omega)$  is the Bose factor, and  $2W(Q) \sim Q^2\gamma(0)$  is the Debye-Waller factor (DWF). With 4.7-Å incident neutrons, NSE offers a  $0.003 \leq t \leq 1$  ns ( $0.6 \leq \omega \leq 200$  μeV) window. Excitations above 200 μeV, but within the 3-meV instrumental bandpass, are revealed by an initial  $S(Q,t)$  below 1.0 (see, e.g., Fig. 2).

To fit the data we use a convenient function (similar to that used by Courtens *et al.*<sup>22</sup>) that has the required limits,

$$g(\omega) = \frac{\omega^2}{(\omega_0^2 + \omega^2)^{(3-d)/3}}. \quad (4)$$

Equation (4) is consistent with sound waves [ $g(\omega) \sim \omega^2$ ] for  $\omega < \omega_0$  and fractons [Eq. (1)] for  $\omega > \omega_0$ . Functions with sharper crossovers were also investigated and lead to similar conclusions.<sup>21</sup> The DWF is determined by the large- $t$  limit of (2), whereas the exponent  $d$  is determined by the initial decay.

Figure 2 shows the observed  $S(Q,t)$  at 300 K. The lines are fits by (2), (3), and (4) to a full  $T$ -dependent data set. The inset shows the corresponding  $g(\omega)$  for

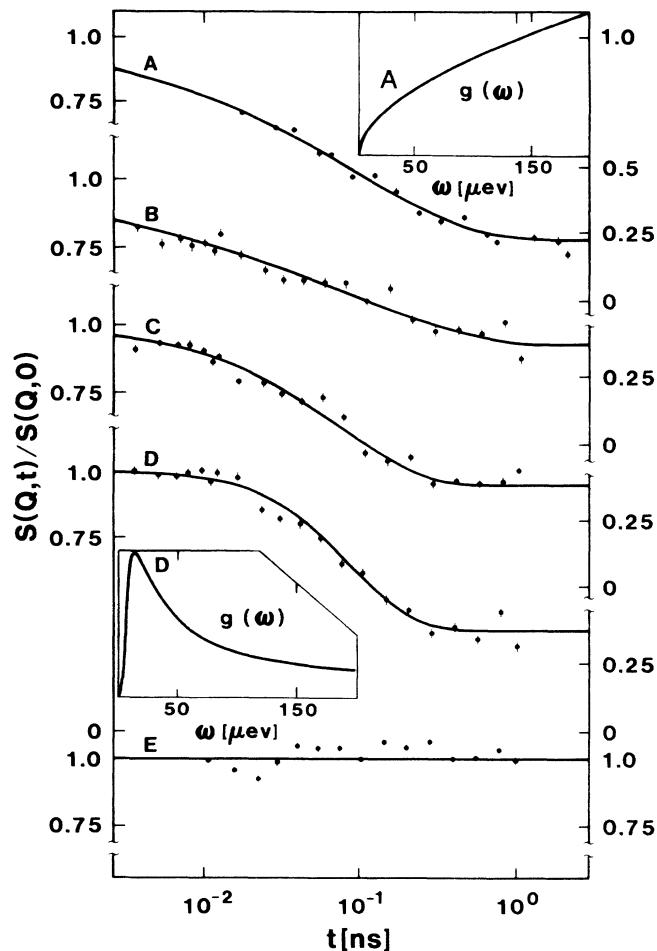


FIG. 2. Measured  $S(Q,t)$  for all samples compared at 300 K. The fits shown were obtained from a simultaneous minimization of a family of  $T$ -dependent runs on each sample assuming  $d$ ,  $\omega_0$ , and  $W/T$  are temperature independent. Inset: The DOS for  $A$  (fracton) and  $D$  (peaked) distributions.

two samples. The parameters associated with the lines are collected in Table I. The DWF is linear in  $T$  indicating harmonic excitations. The observation of fractonlike excitations in the polymeric samples,  $A$ - $C$ , along with the qualitative change in the excitation spectrum with microstructure is the central result of our experiment.

The two polymeric aerogels ( $A, B$ ) exhibit exceedingly broad excitations.  $S(Q,t)$  commences considerably below 1 indicating that a significant fraction of the excitations lies outside the observation window. The higher value of  $d$  for  $B$  compared to  $A$  is consistent with expected increased network ramification. At the same time, the smaller DWF points toward stiffening. The value of  $d$ , however, is not consistent with either scalar ( $d = \frac{4}{3}$ ) or vector ( $d = 0.9$ ) percolation predictions, indicating either superthreshold bond probabilities or complete inadequacy of the kinetic percolation model on large length scales (see next paragraph).

A calculation of the connectivity correlation range  $\xi_c$  from  $\omega_0$  and the velocity of sound ( $\sim 200$  m/s) indicates that  $\xi_c$  exceeds the static correlation range  $\xi$  ( $\xi$  is measured by SAS at small  $Q$ ) by at least an order of magnitude. This discrepancy can be understood from the solution growth data which show that  $\xi$  saturates at about 100 Å before gelation. The growing clusters form a semidilute solution with gelation occurring by formation of links between overlapped clusters. Thus  $\xi_c$  is the mean connectivity length of the clusters at gelation. This size substantially exceeds  $\xi$  which is determined by cluster overlap. The discrepancy between  $\xi_c$  and  $\xi$  appears similar to that reported by Courtens, Vacher, and Stoll<sup>12</sup> based on Brillouin data. Anomalous Brillouin scattering, however, does not require fracton excitations, so we accept the argument of Courtens, Vacher, and Stoll that the Brillouin data are probably explained by simple numeric factors rather than differences between structure and connectivity.

Comparison of  $A$  and  $C$  indicates that pyrolysis leads to a loss of higher-frequency excitations, larger  $\omega_0$ , and a smaller DWF.  $S(Q,t)$  starts close to 1—only a small fraction of the low-frequency spectrum lies outside our dynamic range. These observations imply increased stiffness. The decrease in  $d$ , however, indicates decreased connectivity (or a transition to a peaked excitation spectrum, see below). An explanation of this seemingly inconsistent behavior may be that weak links in the network are sacrificed to enhance molecular-level branching leading to local stiffness but decreased long-range connectivity.

For nonpolymeric samples, we observe qualitatively different behavior. The excitations are completely ab-

TABLE I. Measured parameters of aerogels. Errors are twice the statistical error arising in the fitting procedure. The Porod slope is the limiting value indicated by the lines in Fig. 1.

Code	Class	Porod slope	Density (g/cm <sup>3</sup> )	$d$	$\omega_0$ ( $\mu\text{eV}$ )	$10^3 \times 2WS(Q)/T$ (K <sup>-1</sup> )
$A$	Two-stage	$2.4 \pm 0.1$	0.16	$1.54 \pm 0.09$	$2.0 \pm 0.5$	$4.9 \pm 0.3$
$B$	Single-stage	$2.9 \pm 0.2$	0.15	$1.70 \pm 0.06$	$1.0 \pm 1.4$	$3.2 \pm 0.6$
$C$	Pyrolyzed	$2.5 \pm 0.2$	0.19	$1.22 \pm 0.14$	$5.4 \pm 2.8$	$3.1 \pm 0.4$
$D$	Colloidal	$4.0 \pm 0.5$	0.19	$0.14 \pm 0.28$	$9.0 \pm 2.8$	$3.2 \pm 0.4$
$E$	Sintered	$4.0 \pm 0.4$	...	...	...	...

sent for the sintered material ( $E$ ) even though this material is quite porous at the 100-Å level. More striking, however, is the form of  $S(Q,t)$  for the colloidal microstructure ( $D$ ). Compared to the four-decade decay of  $S(Q,t)$  for the polymeric aerogels, the decay for the colloidal material occurs over one decade, consistent with strong excitations centered around 20  $\mu\text{eV}$ . Furthermore,  $d$  is near zero implying a peak in  $g(\omega)$  (see lower inset, Fig. 2). The peak is at far too low energy to be a "particle model," so we associate it with the excitations of an aggregatelike network of particles.

Based on the above observations we conclude that fracton excitations are only found in polymeric networks. For colloidal microstructures, low-energy excitations are evident, but the broad fracton spectrum is replaced by excitations centered in the 20- $\mu\text{eV}$  regime.

We thank Carol Ashley for synthesis of the polymeric materials and Scott Reed, Ed Vernon, and Barry Ritchie for sample preparation. We thank Bernard Olivier, Phil Seeger, and Steven Spooner for essential contributions to the SAS experiments. This work was performed by the U.S. Department of Energy under Contract No. DE-AC04-76DP00789 for the Office of Basic Energy Sciences, Division of Materials Science.

<sup>1</sup>W. A. Phillips, Rep. Prog. Phys. **50**, 1657 (1987).

<sup>2</sup>*Amorphous Solids—Low Temperature Properties*, edited by W. A. Phillips, Topics in Current Physics Vol. 24 (Springer-Verlag, Berlin, 1981).

<sup>3</sup>U. Buchenau, N. Nucker, and A. J. Dianoux, Phys. Rev. Lett. **53**, 2316 (1984).

<sup>4</sup>T. Freltoft, J. Kjems, and D. Richter, Phys. Rev. Lett. **59**, 1212 (1987).

<sup>5</sup>A. Boukenter, B. Champagnon, E. Duval, J. Dumas, J. F. Quinson, and J. Serughetti, Phys. Rev. Lett. **57**, 2391 (1986).

<sup>6</sup>E. Courtens and R. Vacher, Proc. Roy. Soc. London A **423**, 55 (1989).

<sup>7</sup>Y. Tsujimi, E. Courtens, J. Pelous, and R. Vacher, Phys. Rev. Lett. **60**, 2757 (1988).

<sup>8</sup>F. Mezei, in *Neutron Spin Echo*, edited by F. Mezei, Lecture Notes in Physics Vol. 128 (Springer-Verlag, Berlin, 1979), p. 3.

<sup>9</sup>S. Alexander and R. Orbach, J. Phys. Lett. **43**, L625 (1982).

<sup>10</sup>O. Entin-Wohlman, R. Orbach, and G. Polatsek, in *Dynamics of Disordered Materials*, edited by D. Richter, A. J. Dianoux, W. Petry, and J. Teixeira, Springer Proceedings in Physics Vol. 37 (Springer-Verlag, Berlin, 1989), p. 288.

<sup>11</sup>D. W. Schaefer, J. Phys. (Paris) Colloq. **50**, C4-121 (1989).

<sup>12</sup>E. Courtens, R. Vacher, and E. Stoll, Physica (Amsterdam) **38D**, 41 (1989).

<sup>13</sup>E. Courtens, J. Pelous, J. Phalippou, R. Vacher, and T. Woignier, Phys. Rev. Lett. **58**, 128 (1987).

<sup>14</sup>R. Vacher, E. Courtens, G. Coddens, J. Pelous, and T. Woignier, Phys. Rev. B **39**, 7384 (1989).

<sup>15</sup>G. Reichenauer, J. Fricke, and U. Buchenau, Europhys. Lett. **8**, 415 (1989).

<sup>16</sup>H. Conrad, G. Reichenauer, and J. Fricke, in *Dynamics of Disordered Materials* (Ref. 10), p. 304.

<sup>17</sup>C. J. Brinker, K. D. Keefer, D. W. Schaefer, and C. S. Ashley, J. Non-Cryst. Solids **48**, 47 (1982).

<sup>18</sup>D. W. Schaefer and K. D. Keefer, Phys. Rev. Lett. **53**, 1383 (1984).

<sup>19</sup>D. W. Schaefer, J. P. Wilcoxon, K. D. Keefer, B. C. Bunker, R. K. Pearson, I. M. Thomas, and D. E. Miller, in *Physics and Chemistry of Porous Media II*, edited by J. R. Banavar, J. Koplik, and K. W. Winkler, AIP Conference Proceedings No. 154 (American Institute of Physics, New York, 1986), p. 1.

<sup>20</sup>D. W. Schaefer, C. J. Brinker, J. P. Wilcoxon, D. Q. Wu, J. C. Phillips, and B. Chu, in *Better Ceramics Through Chemistry III*, edited by C. J. Brinker, D. E. Clark, and D. R. Ulrich, MRS Symposia Proceedings No. 121 (Materials Research Society, Pittsburgh, PA, 1988), p. 691.

<sup>21</sup>D. Richter, B. Frick, B. Farago, D. W. Schaefer, and J. C. Brinker (to be published).

<sup>22</sup>E. Courtens, R. Vacher, J. Pelous, and T. Woignier, Europhys. Lett. **6**, 245 (1988).